Environmentally induced lipidome adaptation in the bacterial model organism *M. extorquens*

Grzegorz Chwastek [1], Michal A. Surma [2,3,] ORCID, Sandra Rizk [1,] ORCID, Daniel Grosser [4], Oksana Lavrynenko [5], Magdalena Rucińska [1], Helena Jambor [6,] ORCID, James Sáenz [1,*,] ORCID

1 Technische Universität Dresden, B CUBE, Tatzberg 41, Dresden, DE

2 Lipotype GmbH, Tatzberg 47, Dresden, DE

3 Łukasiewicz Research Network – PORT Polish Center for Technology Development, Stabłowicka 147, Wrocław, PL

4 DZD-Paul Langerhans Institute Dresden, Fetscherstraße 74, Dresden, DE

5 Max Planck Institute of Molecular Cell Biology and Genetics, Pfotenhauerstraße 108, Dresden, DE

6 Technische Universität Dresden, Medizinische Fakultät, Fetscherstraße 74, Dresden, DE

* corresponding author and lead contact: james.saenz@tu-dresden.de

Keywords: Lipidome adaptation, Membrane bioengineering, Lipidome resource, Bacterial-host interactions

Abstract

Cells, from microbes to man, adapt their membranes in response to the environment to maintain their properties and functions. To adapt, lipid composition is homeostatically regulated to conserve optimal membrane properties. Global patterns of lipidome remodelling are poorly understood, particularly in model organisms with simple lipid compositions that can provide insight into fundamental principles underlying membrane adaptation. Using shotgun lipidomics, we examined the simple yet adaptive lipidome of the plant-associated Gram-negative bacterium *Methylobacterium extorquens* over varying temperature, hyperosmotic and detergent stress, carbon sources, and cell density. We observed that as few as ten lipids account for 90% of the total changes, thus constraining the upper limit of variable lipids required for an adaptive living membrane. Across all conditions, the highest degree of lipidomic variability was observed for changing growth temperature. We also revealed that variations in lipid structural features are not monotonic over a given range of conditions and are heterogeneous across lipid classes. Interestingly, phosphotidylcholine showed the most extreme acyl chain remodeling among all lipid classes, suggesting a new link to its importance in bacterial-host interactions and pathogenicity. These patterns in lipidomic remodeling suggest a highly adaptive mechanism with many degrees of freedom and constrain the lipidomic requirements for an adaptive membrane.

1. Introduction

All organisms have at least one membrane that is crucial for compartmentalizing and coordinating biochemical processes within the cell. And yet, nearly a century since the discovery that membranes are made of a lipid bilayer (Gorter and Grendel, 1925) and half a century since integral membrane proteins were proposed in the Fluid Mosaic model (Singer and Nicolson, 1972) we still lack fundamental insight into the design principles required to engineer a functional cell membrane. Much of the membrane's functionality is associated with the activity of membrane proteins, which perform a diverse range of tasks from signaling to transport. The activity of such proteins is in turn crucially dependent on the biophysical properties of the membrane such as viscosity, thickness, curvature and bilayer asymmetry (Hunte and Richers, 2008; Klose et al., 2013; Pomorski and Menon, 2006; Sanders and Mittendorf, 2011). These properties are largely dictated by membrane lipids (Ernst et al., 2016; van Meer et al., 2008).

Cells produce many lipids with different structures that, in their unique combinations, determine the membrane's biophysical state. Moreover, cellular lipidomes can vary from tens, for example in the bacterial lipidome reported here, to hundreds of individual lipid species in mammalian cells (Sampaio et al., 2011; van Meer et al., 2008). A major challenge in membrane research is, therefore, to understand how cells regulate individual lipid abundances to maintain an adaptive, functional membrane. Recent progress reconstituting synthetic membranes from the bottom up is paving the way towards the goal of building a self-sustaining adaptive membrane and presently one of the challenges is to implement adaptive lipid remodeling (Brea et al., 2016; Buddingh and van Hest, 2017; Hardy et al., 2015; Tang et al., 2014). Complex lipidomes can be remodeled to modulate collective membrane properties such as viscosity, lipid packing, thickness and phase properties (Klose et al., 2013; Levental et al., 2016). For instance, increasing the proportion of lipids containing double bonds (acyl chain saturation) or changing the number or position of double bonds along the phospholipid acyl chains, can alter the overall membrane viscosity (Fan and Evans, 2015; Ma et al., 2015; Quinn, 1981; Sinensky, 1974).

Singular observations of lipidome composition do not inform which properties the cell membrane senses and adapts to, nor which minimal suite of lipid structure are required for swift adaptation. Lipidomics has provided global insights into the complexity of cellular lipidomes from yeast to man and can provide insight into how cells remodel lipid composition during adaptation (Ejsing et al., 2009). To date, however, there still are only few studies systematically characterizing lipidomic remodeling across a range of conditions and stressors. The most comprehensive study of this kind

was performed on yeast (Klose et al., 2012), whose lipidome contains over 150 unique lipids, providing unprecedented insight into the adaptation of a complex eukaryotic lipidome.

Complex organisms possess membranes with diverse and niche-specific functional requirements. While understanding complex lipidomes is important, such systems are not ideal for exploring the fundamental principles underlying lipidome adaptation. Since all membranes require means to homeostatically adapt to perturbations (Kaiser et al., 2011), a simpler organism that is capable of adapting to a broad range of environmental conditions would be a more suitable model system to elucidate the minimal lipidomic requirements for adaptation. Bacteria are an attractive target for this endeavor since some are among the simplest organisms, capable of surviving over a broad range of environments, and many species have been well-characterized and established as model organisms for cell biology.

Here, we characterized the lipidomic adaptivity of the Gram-negative bacterium *Methylobacterium extorquens*. *M. extorquens* has a small lipidome, with 25 phospholipid species as compared with over 100 in *E. coli* (Jeucken et al., 2019). Despite its relatively small lipidome, as a plant- and soil-associated bacterium, *M. extorquens* must adapt to a broad range of chemical and physical conditions (Vorholt, 2012). Furthermore, as a eukaryote-associated bacterium with potential for industrial production of chemicals from methanol, understanding lipidome adaptation in Methylobacterium has broad relevance from bacterial-host interactions to bioengineering. We explored lipidomic remodeling over varying temperature, osmotic and detergent stress, carbon source, and cell density. Surprisingly, we find that most lipidome features remain stable, with only minimal modulations even under significant perturbations. However, other lipidome features are highly plastic and contribute to membrane adaptation. Analysis of structural features such as saturation, acyl chain length or headgroup type revealed signatures of adaptive lipidomes. Globally, we observed that as few as 10 lipids, less than half of all available species, account for the majority of lipidomic adaptation across all perturbations. The patterns of lipidome remodeling that we report here provide a resource for exploring the minimal design principles of living membranes and for designing an adaptive synthetic membrane.

100 **2. Results and Discussion**

101

102 **2.1 Experimental Design**

103 To determine lipidomic remodeling induced by environmental perturbations, we measured the
104 lipidomes of *M. extorquens* under physical and chemical challenges to cellular membrane
105 homeostasis (Figure 1a; Figure 1-Figure supplement 1). To this end, we varied temperature, osmotic
106 conditions, detergent stresses, carbon sources, and cell densities (Figure 1-Figure supplement 2).
107 Cells were harvested during early exponential growth to minimize their impact on media chemical
108 composition. Temperature was varied from 6 to 30 ˚C to challenge the viscosity of the membranes.
109 Salt (NaCl) and detergent (Triton X-100) concentrations were varied to produce osmotic and
110 detergent stresses, respectively. Cells were grown on two concentrations of methanol (0.1 and 1%
111 v/v) as the sole carbon source to evaluate the effect of metabolism on lipidomic remodeling. Finally,
112 to characterize lipidomic adaptation at varying cell densities, cells were harvested at early, mid and
113 late exponential, as well as stationary growth stages (Figure 1b). Cellular lipid content was analyzed
114 by high resolution shotgun mass spectrometry (Ejsing et al., 2009) to determine absolute abundances
115 of 25 phospholipids and two hopanoid species, distributed between 5 lipid classes and representing
116 over 90 mol% of the lipidome of *M. extorquens* (Sáenz et al., 2015)(Figure 2).

117

118 It has been previously shown that *M. extorquens* produces predominately lipids with 16 and 18 carbon
119 atoms-long acyl chains, and with up to 2 double bonds per acyl chain (Bradley et al., 2017; Wallace
120 et al., 1990). Consistently, the major PG, PE, and PC species have cumulative chain length of 36 or
121 34 carbons with two double bonds per lipid (e.g. 18:1/18:1 and 18:1/16:1) and minor species with up
122 to 4 double bonds per lipid. We also observed methylation of diplopterol (2Me-DIP) which has
123 previously been reported in cyanobacteria and methylotrophic bacteria including *Methylobacterium*
124 (Bradley et al., 2017; Rashby et al., 2007; Stampf et al., 1991; Summons et al., 1999). Recent work
125 suggests that 2-methylation may be particularly prevalent among plant-associated bacteria (Ricci et
126 al., 2014). In the following sections, we dissect the data in Figure 2 in order to reveal patterns in
127 lipidomic variation across experimental conditions.

128

129 **2.2 Lipidomic variation across experimental conditions**

130 To broadly characterize the effect of environmental perturbations on membrane remodeling, we
131 evaluated the cumulative lipid variability for each growth condition. Presently there is no gold
132 standard for evaluating lipidomic variability. Lipid variability has previously been reported as the
133 variance over mean of lipid abundance (Klose et al., 2012). This analysis reveals how much a lipid

134 varies relative to its abundance, such that even a very low abundance lipid that has a small change in
135 relation to a total lipidome could have a high variance over mean. However, in this study we aimed
136 to characterize variations that would have an impact on the bulk adaptive properties of the membrane.
137 Since small changes in abundance do not have a considerable effect on the bulk adaptive properties
138 of the membrane, we focused on lipids with high absolute changes in abundance. Therefore, we
139 calculated lipid variability as the standard deviation of abundances over a range of conditions. The
140 total lipidomic variability was then calculated as the aggregate standard deviation of relative
141 abundance for all individual lipid species over the range of the various conditions (e.g. temperature,
142 growth stage, etc.) (Figure 3a). This analysis revealed that temperature has by far the largest effect
143 on lipidomic remodeling, with more than 2-fold more variability than any other condition.
144 Surprisingly, the smallest effects were observed with detergent challenge.
145
146 To compare general lipidomic features for each individual experimental condition, we performed a
147 principle component analysis (PCA) on lipid species abundances (Figure 3b). PCA is a method that
148 allows for the comparison of multidimensional data by reducing variations down to two-dimensions
149 called principle components. Distance between each point on the PCA plot is proportional to variation
150 in lipid composition between conditions. Most conditions clustered closely with the standard growth
151 condition, shown in red. Thus, lipid composition was not strongly affected by detergent, methanol,
152 low salt concentrations, or during the progression through early, mid, and late growth stage. In stark
153 contrast, bacteria grown at low temperatures, in stationary growth phase, or at high salt conditions
154 (0.2 M NaCl) did not cluster with the standard growth condition, indicating a high extent of lipidome
155 remodeling. Furthermore, temperature had an orthogonal effect compared to stationary growth and
156 high salt conditions, indicating that a different set of lipidomic features is involved in responses to
157 those conditions.
158
159 It is surprising that a membrane destabilizing detergent (Helenius, 1975) did not result in lipidomic
160 remodeling. This could possibly be attributed to the ability of Gram-negative bacteria to resist
161 chemicals through the robustness imparted by barrier function of lipopolysaccharide at the cell
162 surface and active removal of toxins by multidrug transporters (Nikaido, 1996; 2003; Nikaido and
163 Vaara, 1985; Piddock, 2006). The insensitivity of the lipidome to methanol was also unexpected.
164 Klose et al. (2012) showed that the yeast lipidome varied greatly with differing carbon substrates
165 based on a similar PCA analysis. Our result suggests that methanol and succinate metabolism do not
166 require different membrane properties in *M. extorquens*. Nonetheless, the dominant effect of
167 temperature is consistent with the large diurnal temperature variations that *M. extorquens* must adjust

168 to in its native habitat on plant leaf surfaces and in soils. It is possible that the mechanisms of lipidome
169 adaptation and the lipidomic composition in *M. extorquens* have evolved to be particularly well-
170 suited for temperature changes.
171
172 **2.3 Variation in individual lipid species**
173 We next examined the individual lipid species involved in membrane adaptation in *M. extorquens*
174 (Figure 4). We again calculated individual lipid species as the standard deviation of abundances for
175 a given range of conditions (Figure 4b'). The highest abundance species generally show the largest
176 degree of variability (Figure 4a and 4b). However, there are some low abundance species that exhibit
177 large variations, notably lipids with 3 and 4 double bonds. An important point of emphasis is that low
178 abundance or undetectable species at standard growth conditions can become major components
179 under certain conditions, playing a crucial role in adaptation. The most striking result is that the
180 majority of lipid species do not vary substantially under any conditions, suggesting that only a small
181 fraction of the lipidome is required for adaptive membranes.
182
183 We then asked how many and which lipid species are highly variable for each set of conditions. We
184 defined the highly variable lipid species as those that account for 90% of the total lipidomic variability
185 within any given condition. By this measure we observed that 10-13 lipids are highly variable over
186 any given condition (Figure 4c), meaning that only around 30% of the lipidome is involved in
187 remodeling during adaptation. Of these 10-13 highly variable lipids, 8 are highly variable over all of
188 the conditions tested. These results revealed that only a fraction of the lipidome is involved in adaptive
189 remodeling and point towards the minimum complexity of lipid species required for membrane
190 adaptation. In principle, it is possible that as few as 8 lipid species could support adaptation over the
191 range of experimental conditions examined in this study.
192
193 **2.4 Variation of lipid structural features**
194 Membrane biophysical properties are modulated by changes in the abundance of lipid structural
195 features. For instance, increasing the number of double bonds per lipid reduces membrane viscosity
196 during adaptation to decreasing temperature, whereas various lipid headgroups can impart curvature
197 or surface charge. We analyzed how the various structural features of *M. extorquens* lipids are
198 modulated to glean insight into their sense and response mechanisms of membrane adaptation.
199
200 Headgroup features were differently regulated, as PC, PE and PG were relatively plastic, whereas CL
201 and diplopterols are relatively invariant (Figure 5a). For acyl chains, most of the variability is

202 observed for lipids with 2 and 3 double bonds and with total chain length of 34-36 carbons (Figure
203 5b). When we group acyl chain features separately for each headgroup (e.g. PC-specific unsaturation)
204 PC shows the largest variability for both unsaturation and chain length, whereas PG acyl chain
205 features are nearly invariant. This shows that acyl chain features are regulated independently within
206 each headgroup and provides a starting recipe for designing a responsive synthetic lipidome.
207
208 To assess how much different features varied for each experimental condition we calculated the
209 variance of lipid features for each range of conditions as depicted by the heat map in Figure 5c. The
210 highest variation in lipid classes is observed over temperature and growth stage. Interestingly, total
211 lipid unsaturation varies over temperature but is relatively invariant over all other conditions. The
212 most variation in total lipid chain length varies with temperature and salt concentration. These results
213 reveal that membrane adaptation of total lipid features exhibit different patterns in response to
214 different experimental conditions. This shows that the lipidomic adaptation mechanism is capable of
215 unique, orthogonal responses to different perturbations.
216
217 **2.5 Progressive remodeling of lipids across experimental conditions**
218 Assessing lipidomic data for each step within each condition allows us to compare lipids as we go
219 stepwise through the changes. For instance, how does the lipidome compare when the growth
220 temperature is lowered from 30 to 20 to 13 and to 4 ˚C, or as cells progress from early to mid, to late
221 and finally to stationary growth phase? We again consider lipids grouped by their features as this
222 allowed us to monitor structural variations that directly impact the membrane's biophysical properties
223 (Figure 6; Figure 6-Figure supplement 1-4).
224
225 *Class*
226 Lipid class abundances are relatively invariant over most conditions (Figure 6). PC abundance
227 increases with decreasing temperature, with a pronounced change at 6 ˚C. PE abundance increases
228 considerably when cells are in stationary growth stage. These results suggest that lipid class
229 distribution is only adjusted under extreme conditions.
230
231 *Double Bonds*
232 The total number of double bonds per lipid varies substantially with temperature and is nearly
233 invariant for other conditions (Figure 6a). As temperature decreases the abundances of DB3 and DB4
234 lipids increase, while abundances of DB1 and DB2 decrease. This contrasts with other organisms
235 such as yeast where primarily DB1 and DB2 are adjusted with temperature change (Klose et al.,

236 2012). It is possible that having additional double bonds enhances Methylobacterium's ability to
237 adapt to broad temperatures that they experience on plant surfaces and in soils.
238
239 The variation of double bonds per lipid within each headgroup class is not evenly distributed across
240 classes (Figure 6b). For instance, for varying temperatures PC shows the highest remodeling whereas
241 PG is nearly invariant. Additionally, for varying salt and growth stages where total unsaturation has
242 little or negligible variability, class-specific PC-DB and CL-DB vary considerably. These variations
243 in PC-DB and CL-DB are nearly equal and opposite resulting in no apparent change in total DB
244 content.
245
246 *Chain length*
247 Total chain length is highly conserved across all conditions, and only varies substantially at 6 ˚C
248 (Figure 6a). Since total chain length has a large effect on membrane thickness, which in turn must be
249 matched with membrane proteins transmembrane domain length, it is not surprising that this feature
250 is so invariant. The large change in total CL at extreme low temperature suggests that the membrane
251 must take extreme measures to adapt as it approaches the end of the range of viable growth
252 temperature.
253
254 Similar to unsaturation, chain length within each headgroup class shows much higher variability than
255 total chain length (Figure 6b). For instance, from 30 to 20 ˚C total chain length remains constant
256 while PC chain length decreases and is compensated for by increased chain length in PG, PE and CL.
257 Similar remodeling is also observed for growth stage and salt concentration. Additionally, PC exhibits
258 the highest chain length variation.
259
260 *Diplopterol 2-methylation*
261 A particularly striking variation was observed for the sterol analogue diplopterol and its 2-methylated
262 derivative (Figure 7). Diplopterol is the major hopanoid in *M. extorquens* and is localized in the outer
263 membrane (Hancock and Williams, 1986; Sáenz et al., 2015). We previously demonstrated that
264 diplopterol has a sterol-like ability to modulate the order of saturated lipids such as
265 lipopolysaccharides in the bacterial outer membrane (Sáenz et al., 2015; 2012). Subsequent work
266 demonstrated that 2-methylation of hopanoids increases their membrane rigidifying effect (Wu et al.,
267 2015). Therefore, variations in diplopterol 2-methylation could play a role in the adaptation of the
268 outer membrane. While total diplopterol abundances (diplopterol + 2-methyl-diplopterol) did not
269 vary substantially under any conditions, 2-methylation of diplopterol is highly variable in all

conditions except methanol and detergent (Figure 7a and b). There is a progressive increase in 2-methyl-diplopterol abundance with decreasing temperature and increasing salt concentration (Figure 7c), consistent with transcriptional regulation of this process by global stress response pathways (Kulkarni et al., 2013). These results show for the first time that 2-methylation is dynamically regulated in response to varying growth conditions and is important for outer membrane adaptation.

Our observations highlight three characteristics of structural lipid adaptation. First, we observed that adaptivity of features over a particular range of conditions (e.g. temperature) does not involve a monotonic pattern of feature remodeling, but rather can involve different features over intervals of a given condition. Second, certain features such as acyl chain unsaturation and diplopterol 2-methylation are highly variable and are remodeled over a broad range of conditions. However, other features such as lipid class and acyl chain length are relatively invariant except under extreme conditions of low temperature and stationary growth stage, suggesting that chain length and headgroup distribution have multiple constraints (e.g. maintaining membrane thickness or surface charge). Notably, even the tightly constrained features are adjusted under extreme perturbations. Third, acyl chain features are regulated independently within each headgroup class. Thus, even when total acyl chain unsaturation and length appears invariant, there can be extensive acyl chain remodeling within specific headgroup classes. Such class-specific remodeling of unsaturation may result in adaptation that is localized to the inner or outer membrane, or to specific regions within each membrane, such as highly curved regions at the poles, one particular membrane leaflet, lipids that are closely associated with protein transmembrane domains, or potentially lateral membrane domains. On the other hand, constraining total unsaturation while internally shifting double bonds from PC to CL might be a means of varying intrinsic curvature while maintaining total membrane viscosity.

Summary and Outlook

In this study, we systematically characterized the lipidome of *M. extorquens* over a range of growth conditions to gain insights into membrane homeostatic adaptation. Countless studies have addressed phospholipid acyl chain composition (e.g. as measured by GC or GC-MS) and have revealed an important role of membrane lipid composition to various phenotypic aspects. However, phospholipid headgroups and acyl chains jointly determine membrane properties. Using shotgun lipidomics, we provide a near-complete lipidome down to the species level. This allowed us to map how structural features of lipids (e.g. head group, saturation, chain length) are recombined to achieve adaptation. We demonstrated that membranes composed of only a few lipid species are capable of adapting specifically to a broad range of conditions, in particular temperature. Additionally, by assessing how

304 lipid structural features are recombined through adaptation, we reveal that even a simple lipidome
305 exhibits complex patterns of remodelling that were previously undefined. We propose that it is
306 essential to assess lipidomic data in terms of the composite structural features conferred by binned
307 combinations of lipids, since the combination of these structural features ultimately dictates the
308 physical state and functionality of membranes.
309
310 We probed the lipidome composition across a broad range of viable conditions spanning temperature,
311 hyperosmotic and detergent stress, carbon sources, and cell density. PCA analysis revealed that most
312 lipidomes are highly similar across conditions (Figure 3). This demonstrates that the lipidome is
313 robust and that there are strong constraints on lipidome composition and remodelling. While
314 individual lipid species do adapt to changing conditions, eight lipid species are variable in all
315 experimental regimes (Figure 4) and the majority of lipids remained surprisingly stable. One of the
316 outstanding conundrums in membrane biology is to understand why there are so many lipids
317 (Dowhan, 1997; 2017), even a relatively simple organism like *E. coli* has over 100 phospholipid
318 species (Jeucken et al., 2019). Recapitulating such a complex system from first principles seems
319 daunting. However, the lipidome of *M. extorquens* demonstrates that a synthetic membrane capable
320 of supporting life over a broad range of environmental conditions could be constructed with a
321 relatively small number of lipid species.
322
323 Lipidome adaptation is also constrained by structural elements of individual lipids. Instead of
324 analysing lipidomes purely by lipid species, it is therefore critical to assess global structural
325 composition. For example, total phospholipid chain length, that influences membrane thickness, is a
326 highly conserved feature that only varies under extreme conditions such as low temperature (Jensen
327 and Mouritsen, 2004). Interestingly, phospholipid acyl chain length was highly conserved globally,
328 but variable within certain headgroup classes. Other constraints do not have such clear implications.
329 For instance, phospholipid headgroup composition only varies at low temperature or in stationary
330 growth phase, possibly suggesting conservation of membrane surface charge as a key constraint.
331 Also, the acyl chain composition among phospholipids with PG headgroup is nearly invariant across
332 all conditions, suggesting that there could be biochemical constraints on PG remodelling. Low PG
333 remodelling has also been observed in cyanobacteria (Pittera et al., 2018), showing that this constraint
334 is not limited to *M. extorquens*. While the physicochemical and physiological basis for these
335 observations remains to be fully explored, the patterns and constraints in lipidome remodelling that
336 we report here serve as a resource for designing a minimal adaptive membrane and highlight the need
337 for multi-level analysis of lipidome data.

338

339 Among all phospholipid classes, we observed that phosphotidylcholine (PC) showed the highest
340 degree of acyl chain remodelling. This is particularly interesting with regard to bacterial-host
341 interactions. While relatively few bacteria synthesize PC, the majority of studied bacteria associated
342 with a eukaryotic host, including many pathogens, contain PC in their membranes (Aktas et al., 2010;
343 Geiger et al., 2013). Synthesis of PC was previously shown to be essential for host colonization
344 (Minder et al., 2001) and for pathogen virulence (Conde-Alvarez et al., 2006; Wessel et al., 2006).
345 The specific physiological role of bacterial PC, however, is still unclear. Our results that PC accounts
346 for most acyl chain remodelling in *M. extorquens* could suggest a pivotal role of membrane adaptation
347 through PC remodelling for bacterial-host interactions.

348

349 Understanding how *M. extorquens* adapts with so few lipids, and even fewer that are responsive,
350 remains an open challenge. In particular, given that lipid remodelling did not involve a monotonic
351 change, but rather seemed to involve different features varying over different intervals of a given
352 range of conditions, such as temperature. Critical to understanding the mechanisms underlying
353 lipidome adaptation are the sense and response pathways that regulate the remodelling of lipid
354 structural features. It has emerged in recent years that there can be dedicated membrane sensors,
355 which are involved in regulating lipid biosynthesis pathways in response to perturbed membrane
356 properties (Ernst et al., 2016; Puth et al., 2015; Saita and de Mendoza, 2015). Recently, it was
357 demonstrated that in addition to membrane thickness and viscosity, some membrane sensors are
358 poised to detect changes in lateral tension in the bilayer (Ballweg et al., 2019), suggesting a diverse
359 range of possible inputs to lipidome adaptation. Building on the lipidomic resource presented here,
360 *M. extorquens* is a promising model organism to explore minimal mechanisms for cell membrane
361 adaptation. The adaptive lipidome of *M. extorquens* provides a critical resource as a starting point to
362 elucidate the regulatory systems underlying membrane adaptation.

363

364 **Acknowledgements**

365 The authors wish to thank Kai Simons and Robert Ernst for advice, members of Sáenz group for
366 discussions, Michael Schlierf, Ilya Levental, Alex Bradley, Carl Modes, and Christoph Zechner for
367 manuscript comments, and Lipotype GmbH.

368

369 **Author contributions**

370 Sandra Rizk and Daniel Grosser performed bacterial growth experiments. Oksana Lavrynenko
371 performed MS analysis. Grzegorz Chwastek contributed to writing, editing and data analysis. Michał

Surma performed MS data analysis and editing. Magda Rucińska performed bioinformatics analysis. Helena Jambor conceived and designed the figures. James Sáenz conceived the project, obtained funding, supervised the project, and wrote the manuscript. All authors read, edited and approved the final manuscript.

Funding

This work was supported by the B CUBE of the TU Dresden, a Simons Foundation Fellowship (to JPS), a German Federal Ministry of Education and Research BMBF grant (to JPS, project # 03Z22EN12), and a VW Foundation "Life" grant (to JPS, project # 93089).

382 **Methods**

383

384 **Media, growth conditions**

385 For all cultivations a defined media, here referred to as Hypho-TMM, was used (Delaney et al., 2013).
386 All liquid cultures were grown at 30 ˚C and pH 7 with shaking at 150 rpm unless stated otherwise.
387 For all experiments we used a strain of *M. extorquens PA1* with the cellulose synthase genes knocked
388 out to minimize clumping and improve cell density measurements (Delaney et al., 2013). Cultures
389 were started from a glycerol stock stored at -80 ˚C and were plated on Hypho-TMM agarose plate
390 and grown at 30 ˚C. A liquid pre-culture was set up by sterile picking a single colony and transferring
391 it to 5 ml of Hypho-TMM. This pre-culture was grown over night to near stationary phase. The
392 experimental culture was started by inoculation to $OD_{600\ nm}$ 0.02 with pre-culture and grown until a
393 final $OD_{600\ nm}$ of 0.2 – 0.3 (early log-phase) was reached. Several conditions were tested including
394 the influence of salinity, carbon source (MeOH and succinate), detergent (up to 5% Triton X-100)
395 and temperature (6 – 30 ˚C). Cells were also harvested at mid-, late- and stationary growth stages. A
396 defined volume representing 6 OD units (1 OD unit = 1 mL of OD 1) was sampled and pelleted. The
397 harvested cells were washed twice with fresh media. The pellet was snap frozen in liquid nitrogen
398 and stored until further processing at -20 ˚C.

399

400 *Hypho-TMM recipe:*

401 1.45 mM K_2HPO_4; 1.88 mM NaH_2PO_4; 45.6 µM sodium citrate; 1.2 µM $ZnSO_4$; 1 µM $MnCl_2$;
402 18 µM $FeSO_4$; 2 µM $(NH_4)_6Mo_7O_{24}$; 1 µM $CuSO_4$; 2 µM $CoCl_2$; Na_2WO_4; 0.5 mM $MgCl_2$;
403 8 mM $(NH_4)_2SO_4$; 20 µM $CaCl_2$
404 30 mM PIPES pH 7
405 15 mM succinate unless stated otherwise

406

407 **Shotgun mass spectrometry**

408 For the lipidomic analysis by mass spectrometry the lipids of harvested cells were extracted twice by
409 the method of Blight and Dyer (Bligh and Dyer, 1959). The total lipid extracts representing 6 OD
410 units of *M. extorquens* were analysed by quantitative shotgun lipidomics (Ejsing et al., 2009) adapted
411 for the quantification of hopanoids (diplopterol and 2-methyl-diplopterol).

412

413 *Measurement of phospholipids*

414 For absolute quantification extracts were diluted with MS mix (7.5 mM ammonium acetate in
415 isopropanol/methanol/chloroform 4:2:1) containing the 0.5 µM PC (34:0), PE (34:0), PG (34:0)

416 mixture and 0.05 µM CL (57:4). MS spectra were acquired on Q Exactive tandem mass spectrometer
417 (Thermo Fisher Scientific, Bremen, Germany) equipped with a robotic nanoflow ion source TriVersa
418 NanoMate (Advion BioSciences, Ithaca NY). Spectra were acquired in negative MS mode with the
419 mass resolution of $R_{m/z\ 400}$ = 280000 with AGC target value of 10^6 and maximum injection time of 1
420 s in the range of masses 400 – 1000 m/z. Raw data were processed using LipidXplorer software
421 (Herzog et al., 2012; 2011). Based on high accuracy and resolution masses, species belonging to 4
422 phospholipid classes including phosphatidylcholine (PC), detected as an acetate adduct,
423 phosphatidylethanolamine (PE), phosphatidylglycerol (PG), both detected as deprotonated anions,
424 and cardiolipin (CL), detected as a doubly deprotonated anion, were identified.
425
426 *Measurement of diplopterol*
427 The extract was dried down and re-dissolved in MS mix (7.5 mM ammonium acetate in
428 isopropanol/methanol/chloroform 4:2:1) containing the 0.13 mM cholesterol D7 standard. MS
429 spectra were acquired on Q Exactive tandem mass spectrometer (Thermo Fisher Scientific, Bremen,
430 Germany) equipped with a robotic nanoflow ion source TriVersa NanoMate (Advion BioSciences,
431 Ithaca NY). Spectra were acquired in positive MS mode with the mass resolution of $R_{m/z\ 400}$ = 140000
432 with AGC target value of 10^6 and maximum injection time of 1 s in the range of masses 360 – 455
433 m/z. Raw data were processed using LipidXplorer software. Diplopterol and 2-methyl-diplopterol
434 were detected as M - $[H_2O]$ + H^+ ... and cholesterol D7 as M - $[H_2O]$ + H^+. Absolute concentrations
435 of diplopterol and methyl-diplopterol were determined using calibration curves and response factors
436 established alongside with cholesterol D7 and purified diplopterol mixed at various ratios.
437
438 **Data analysis**
439 Lipid abundances (mol% of total) of biological triplicates for all conditions are provided in the
440 supplementary materials. One of the replicates at 13 ˚C and at TX-100 1% yielded erroneous
441 abundance data due to a problem with the internal standard in those replicates and we have therefore
442 excluded them from our analyses.
443
444 Variation of lipid species across experimental conditions was calculated by taking the standard
445 deviation of lipid abundances for replicates over a given range of conditions (e.g. temperature, salt,
446 etc.). Total lipidomic variation was calculated as the cumulative variation of individual lipid species
447 for a given range of conditions.
448

Visualization of lipidome variation for all conditions was investigated with principle component analysis (PCA). PCA was performed by using the R prcomp function in RStudio with default parameters, where the calculation is carried out by a singular value decomposition of the (centered and scaled) data matrix. Visualization in single plots performed using the ggbiplot function. PCA allows the identification of latent variables (principal components) in the data based on 14 observed variables. The plot is based on principal components 1 and 2, which explain 50.1% and 16.5% of the total variance of the data, respectively.

Variations in abundance of lipid features were analysed by binning lipid species according to structural features including total chain length, saturation, class (e.g. phospholipid headgroup and diplopterols), and 2-methylation of diplopterol. Acyl chain length and saturation were binned for all phospholipids (global acyl chain features), and separately within each headgroup (headgroup specific acyl chain features).

464
465 **Figure Captions**
466
467 **Figure 1. Overview of experimental outline and lipids analysed in this study. (A)** Overview of
468 experimental design and exemplary data obtained. **(B)** Schematic of lipid structural features measured
469 in this study: headgroups of phospholipids and isoprenoids, acyl chain length and acyl chain
470 saturation (number of double bonds).
471
472 **Figure 1-figure supplement 1.** Bacterial growth rates (Herbert et al., 1956) for all experimental
473 conditions.
474
475 **Figure 2. Table of lipid species abundances.** Lipid species are annotated by class/headgroup (PG,
476 PE, PC, CL or diplopterol), total acyl chain length (32 to 72), and total acyl chain saturation (number
477 of double bonds per lipid, 0 to 4). Abundance is shown as percentage of total lipids per experiment.
478 The range in abundance across all experimental conditions is indicated by individual grey dots, the
479 abundances for the standard growth condition (30 ˚C, early exponential stage, 0.15 M sucrose) are
480 shown in red.
481
482 **Figure 3. Effect of experimental conditions on lipidomic variability. (A)** Total lipidomic
483 variability is given as the cumulative standard deviation of individual lipid species across each set of
484 experimental conditions. Lipid variability is highest when varying temperature, and lowest in
485 increasing percentage of detergent. **(B)** Principle component analysis (PCA) of the lipid species
486 abundances shows the degree of variation between subconditions. The standard growth condition (30
487 ˚C, early exponential stage, 0.15 M sucrose) is indicated in red, and all other subconditions are grey.
488 Again, lipidomes vary greatly in changing temperatures regimes, and also when bacteria enter
489 stationary phase growth.
490
491 **Figure 4. Variability of individual lipid species across experimental conditions. (A)** Average
492 abundances of lipid species for all conditions sorted from highest (PG 36:2) to lowest (CL 64:0) lipid
493 species. Mean and range are shown for each lipid. **(B)** Heat map of lipid species variability across
494 experimental conditions, high variability is indicated in red, no variability in light yellow. **(B')**
495 Exemplary calculation of standard deviation. **(C)** UpSetR plot (Conway et al., 2017) showing the
496 overlap of lipids adapting their amounts across the experimental conditions. Eight lipids vary their
497 abundance in all experimental conditions, four lipids vary abundance specifically in changing
498 temperatures. Stage: bacterial growth stage/phase, TX: varying detergent concentrations.
499
500 **Figure 5. Variability of phospholipid structural features across experimental conditions. (A)**
501 Abundances of lipids grouped by lipid class shows overall low variability, and lowest variability of
502 CL. **(B)** Abundances of phospholipid headgroup binned by acyl chain length and acyl chain saturation
503 respectively reveals group specific differences in acyl chain remodeling. (headgroups: blue = PG,
504 green = PE, olive = PC, magenta = CL). **(A), (B)** each data point shows lipid abundance from
505 individual biological replicates. **(C)** Variability of lipid features plotted for each set of experimental
506 conditions. Stage: bacterial growth stage/phase, TX: varying detergent concentrations.
507
508 **Figure 6. Step-wise adaptation of lipids by feature at changing environmental growth**
509 **conditions. (A)** Abundances of lipids grouped by class, acyl chain length and acyl chain saturation
510 when changing growth temperature, probing at different growth stages, and varying salt (NaCl)
511 concentration of the growth media. **(B)** Abundances of phospholipids grouped by acyl chain features,
512 with headgroups indicated by color (blue: PG, green: PE, olive: PC, magenta: CL). This reveals
513 compensatory effects in lipid adaptability: while abundance of PC with 2 double bonds increases with

514 increasing temperatures, PC with 3 double bonds decreases from 6 to 30 ˚C. In each panel, the most
515 variable features are highlighted in bold.
516
517 **Figure 7. Diplopterol (hopanoid) methylation (A)** Abundances of diplopterol species across growth
518 conditions. **(B)** Step-wise adaptation of diplopterols when changing temperature, growth phase, and
519 salt condition.
520
521 **Figure 1 – Supplement 1** Graphical abstract
522 **Figure 1 – Supplement 2** Bacterial growth curves and sampling points for lipidomic analysis. Chart
523 for growth phases is a conceptual drawing.
524 **Figure 6 – Supplement 1** Overview of compositional changes across exemplary experimental
525 conditions reveals the lipidome is robust in most growth conditions except in drastic temperature
526 changes when the lipidome is markedly different.
527 **Figure 6 – Supplement 2.** Step-wise adaptation of lipids by feature sampled at varying growth
528 temperatures.
529 **Figure 6 – Supplement 3.** Step-wise adaptation of lipids by feature sampled at early, late, mid and
530 stationary growth phase.
531 **Figure 6 – Supplement 4.** Step-wise adaptation of lipids by feature sampled at varying salt
532 concentrations (NaCl).
533
534
535
536
537
538
539
540
541

542 **References**
543

544 Aktas, M., Wessel, M., Hacker, S., Klüsener, S., Gleichenhagen, J., and Narberhaus, F. (2010).
545 Phosphatidylcholine biosynthesis and its significance in bacteria interacting with eukaryotic cells.
546 Eur. J. Cell Biol. *89*, 888–894.

547 Ballweg, S., Sezgin, E., Wunnicke, D., Hänelt, I., and Ernst, R. (2019). Regulation of lipid
548 saturation without sensing membrane fluidity. Biorxiv *40*, 706556.

549 Bligh, E.G., and Dyer, W.J. (1959). A Rapid Method of Total Lipid Extraction and Purification.
550 Canadian Journal of Biochemistry and Physiology *37*, 911–917.

551 Bradley, A.S., Swanson, P.K., Muller, E.E.L., Bringel, F., Caroll, S.M., Pearson, A., Vuilleumier,
552 S., and Marx, C.J. (2017). Hopanoid-free Methylobacterium extorquens DM4 overproduces
553 carotenoids and has widespread growth impairment. PLoS ONE *12*, e0173323.

554 Brea, R.J., Rudd, A.K., and Devaraj, N.K. (2016). Nonenzymatic biomimetic remodeling of
555 phospholipids in synthetic liposomes. P Natl Acad Sci Usa *113*, 8589–8594.

556 Buddingh, B.C., and van Hest, J.C.M. (2017). Artificial Cells: Synthetic Compartments with Life-
557 like Functionality and Adaptivity. Acc. Chem. Res *50*, 769–777.

558 Conde-Alvarez, R., Grilló, M.J., Salcedo, S.P., de Miguel, M.J., Fugier, E., Gorvel, J.P., Moriyón,
559 I., and Iriarte, M. (2006). Synthesis of phosphatidylcholine, a typical eukaryotic phospholipid, is
560 necessary for full virulence of the intracellular bacterial parasite Brucella abortus. Cell. Microbiol.
561 *8*, 1322–1335.

562 Conway, J.R., Lex, A., and Gehlenborg, N. (2017). UpSetR: an R package for the visualization of
563 intersecting sets and their properties. Bioinformatics *33*, 2938–2940.

564 Delaney, N.F., Kaczmarek, M.E., Ward, L.M., Swanson, P.K., Lee, M.C., and Marx, C.J. (2013).
565 Development of an optimized medium, strain and high-throughput culturing methods for
566 Methylobacterium extorquens. PLoS ONE *8*, e62957.

567 Dowhan, W. (1997). Molecular basis for membrane phospholipid diversity: why are there so many
568 lipids? Annu Rev Biochem.

569 Dowhan, W. (2017). Understanding phospholipid function: Why are there so many lipids? J. Biol.
570 Chem. *292*, 10755–10766.

571 Ejsing, C.S., Sampaio, J.L., Surendranath, V., Duchoslav, E., Ekroos, K., Klemm, R.W., Simons,
572 K., and Shevchenko, A. (2009). Global analysis of the yeast lipidome by quantitative shotgun mass
573 spectrometry. Proceedings of the National Academy of Sciences *106*, 2136–2141.

574 Ernst, R., Ejsing, C.S., and Antonny, B. (2016). Homeoviscous Adaptation and the Regulation of
575 Membrane Lipids. Journal of Molecular Biology *428*, 4776–4791.

576 Fan, W., and Evans, R.M. (2015). Turning up the heat on membrane fluidity. Cell *161*, 962–963.

577 Geiger, O., Lopez-Lara, I.M., and Sohlenkamp, C. (2013). Phosphatidylcholine biosynthesis and
578 function in bacteria. Biochim Biophys Acta *1831*, 503–513.

579 Gorter, E., and Grendel, F. (1925). On biomolecular layers of lipoids on the chromocytes of the
580 blood. J Exp Med *41*, 439–443.

581 Hancock, I., and Williams, K. (1986). The outer membrane of Methylobacterium organophilum.
582 Microbiology.

583 Hardy, M.D., Yang, J., Selimkhanov, J., Cole, C.M., Tsimring, L.S., and Devaraj, N.K. (2015).
584 Self-reproducing catalyst drives repeated phospholipid synthesis and membrane growth. P Natl
585 Acad Sci Usa *112*, 8187–8192.

586 Helenius, A. (1975). Solubilization of membranes by detergents. Biochim Biophys Acta.

587 Herzog, R., Schuhmann, K., Schwudke, D., Sampaio, J.L., Bornstein, S.R., Schroeder, M., and
588 Shevchenko, A. (2012). LipidXplorer: A Software for Consensual Cross-Platform Lipidomics.
589 PLoS ONE *7*, e29851.

590 Herzog, R., Schwudke, D., Schuhmann, K., Sampaio, J.L., Bornstein, S.R., Schroeder, M., and
591 Shevchenko, A. (2011). A novel informatics concept for high-throughput shotgun lipidomics based
592 on the molecular fragmentation query language. Genome Biol. *12*, R8.

593 Hunte, C., and Richers, S. (2008). Lipids and membrane protein structures. Curr Opin Struct Biol
594 *18*, 406–411.

595 Jensen, M., and Mouritsen, O. (2004). Lipids do influence protein function - the hydrophobic
596 matching hypothesis revisited. BBA-Biomembranes *1666*, 205–226.

597 Jeucken, A., Molenaar, M.R., van de Lest, C.H.A., Jansen, J.W.A., Helms, J.B., and Brouwers, J.F.
598 (2019). A Comprehensive Functional Characterization of Escherichia coli Lipid Genes. Cell Rep
599 *27*, 1597–1606.e2.

600 Kaiser, H.-J., Surma, M.A., Mayer, F., Levental, I., Grzybek, M., Klemm, R.W., Da Cruz, S.,
601 Meisinger, C., Müller, V., Simons, K., et al. (2011). Molecular Convergence of Bacterial and
602 Eukaryotic Surface Order. J Biol Chem *286*, 40631–40637.

603 Klose, C., Surma, M.A., and Simons, K. (2013). Organellar lipidomics-background and
604 perspectives. Curr Opin Cell Biol.

605 Klose, C., Surma, M.A., Gerl, M.J., Meyenhofer, F., Shevchenko, A., and Simons, K. (2012).
606 Flexibility of a Eukaryotic Lipidome – Insights from Yeast Lipidomics. PLoS ONE *7*, e35063.

607 Kulkarni, G., Wu, C.-H., and Newman, D.K. (2013). The General Stress Response Factor EcfG
608 Regulates Expression of the C-2 Hopanoid Methylase HpnP in *Rhodopseudomonas palustris* TIE-1.
609 J Bacteriol *195*, 2490–2498.

610 Levental, K.R., Lorent, J.H., Lin, X., Skinkle, A.D., Surma, M.A., Stockenbojer, E.A., Gorfe, A.A.,
611 and Levental, I. (2016). Polyunsaturated Lipids Regulate Membrane Domain Stability by Tuning
612 Membrane Order. Biophys J *110*, 1800–1810.

613 Ma, D.K., Li, Z., Lu, A.Y., Sun, F., Chen, S., Rothe, M., Menzel, R., Sun, F., and Horvitz, H.R.
614 (2015). Acyl-CoA Dehydrogenase Drives Heat Adaptation by Sequestering Fatty Acids. Cell *161*,
615 1152–1163.

616 Minder, A.C., de Rudder, K.E., Narberhaus, F., Fischer, H.M., Hennecke, H., and Geiger, O.
617 (2001). Phosphatidylcholine levels in Bradyrhizobium japonicum membranes are critical for an
618 efficient symbiosis with the soybean host plant. Mol Microbiol *39*, 1186–1198.

619 Nikaido, H. (1996). Multidrug efflux pumps of gram-negative bacteria. J Bacteriol *178*, 5853–5859.

620 Nikaido, H. (2003). Molecular basis of bacterial outer membrane permeability revisited.
621 Microbiology and Molecular Biology Reviews *67*, 593–656.

622 Nikaido, H., and Vaara, M. (1985). Molecular-Basis of Bacterial Outer-Membrane Permeability.
623 Microbiol Rev *49*, 1–32.

624 Piddock, L.J.V. (2006). Multidrug-resistance efflux pumps - not just for resistance. Nat Rev Micro
625 *4*, 629–636.

626 Pittera, J., Jouhet, J., Breton, S., Garczarek, L., Partensky, F., Maréchal, É., Nguyen, N.A., Doré,
627 H., Ratin, M., Pitt, F.D., et al. (2018). Thermoacclimation and genome adaptation of the membrane
628 lipidome in marine Synechococcus. Environ Microbiol *20*, 612–631.

629 Pomorski, T., and Menon, A.K. (2006). Lipid flippases and their biological functions. Cell Mol Life
630 Sci *63*, 2908–2921.

631 Puth, K., Hofbauer, H.F., Sáenz, J.P., and Ernst, R. (2015). Homeostatic control of biological
632 membranes by dedicated lipid and membrane packing sensors. Biol Chem *396*, 1043–1058.

633 Quinn, P. (1981). The fluidity of cell membranes and its regulation. Progress in Biophysics and
634 Molecular Biology.

635 Rashby, S.E., Sessions, A.L., Summons, R.E., and Newman, D.K. (2007). Biosynthesis of 2-
636 methylbacteriohopanepolyols by an anoxygenic phototroph. Proceedings of the National Academy
637 of Sciences *104*, 15099–15104.

638 Ricci, J.N., Coleman, M.L., Welander, P.V., Sessions, A.L., Summons, R.E., Spear, J.R., and
639 Newman, D.K. (2014). Diverse capacity for 2-methylhopanoid production correlates with a specific
640 ecological niche. The ISME Journal *8*, 675–684.

641 Saita, E.A., and de Mendoza, D. (2015). Thermosensing via transmembrane protein–lipid
642 interactions. Biochimica Et Biophysica Acta (BBA)-Biomembranes *1848*, 1757–1764.

643 Sampaio, J.L., Gerl, M.J., Klose, C., Ejsing, C.S., Beug, H., Simons, K., and Shevchenko, A.
644 (2011). Membrane lipidome of an epithelial cell line. P Natl Acad Sci Usa *108*, 1903–1907.

645 Sanders, C.R., and Mittendorf, K.F. (2011). Tolerance to Changes in Membrane Lipid Composition
646 as a Selected Trait of Membrane Proteins. Biochemistry *50*, 7858–7867.

647 Sáenz, J.P., Grosser, D., Bradley, A.S., Lagny, T.J., Lavrynenko, O., Broda, M., and Simons, K.
648 (2015). Hopanoids as functional analogues of cholesterol in bacterial membranes. P Natl Acad Sci
649 Usa *112*, 11971–11976.

650 Sáenz, J.P., Sezgin, E., Schwille, P., and Simons, K. (2012). Functional convergence of hopanoids
651 and sterols in membrane ordering. Proceedings of the National Academy of Sciences *109*, 14236–
652 14240.

653 Sinensky, M. (1974). Homeoviscous adaptation--a homeostatic process that regulates the viscosity
654 of membrane lipids in Escherichia coli. Proceedings of the National Academy of Sciences *71*, 522–
655 525.

656 Singer, S.J., and Nicolson, G.L. (1972). The fluid mosaic model of the structure of cell membranes.
657 Science *175*, 720–731.

658 Stampf, P., Herrmann, D., Bisseret, P., and Rohmer, M. (1991). 2α-Methylhopanoids: First
659 Recognition in the Bacterium Methylobacterium organophilum and Obtention via Sulphur Induced
660 Isomerization of 2ß-Methylhopanoids. Tetrahedron *47*, 7081–7090.

661 Summons, R.E., Jahnke, L.L., Hope, J.M., and Logan, G.A. (1999). 2-Methylhopanoids as
662 biomarkers for cyanobacterial oxygenic photosynthesis. Nature *400*, 554–557.

663 Tang, D., Rohaida Che Hak, C., Thompson, A.J., Kuimova, M.K., Williams, D.S., Perriman, A.W.,
664 and Mann, S. (2014). Fatty acid membrane assembly on coacervate microdroplets as a step towards
665 a hybrid protocell model. Nature Chemistry *6*, 527–533.

666 van Meer, G., Voelker, D.R., and Feigenson, G.W. (2008). Membrane lipids: where they are and
667 how they behave. Nat Rev Mol Cell Bio *9*, 112–124.

668 Wallace, P., Hollis, D., and Weaver, R. (1990). Biochemical and chemical characterization of pink-
669 pigmented oxidative bacteria. Journal of Clinical ….

670 Wessel, M., Klüsener, S., Gödeke, J., Fritz, C., Hacker, S., and Narberhaus, F. (2006). Virulence of
671 Agrobacterium tumefaciens requires phosphatidylcholine in the bacterial membrane. Mol Microbiol
672 *62*, 906–915.

673 Wu, C.-H., Bialecka-Fornal, M., and Newman, D.K. (2015). Methylation at the C-2 position of
674 hopanoids increases rigidity in native bacterial membranes. eLife *4*.

675

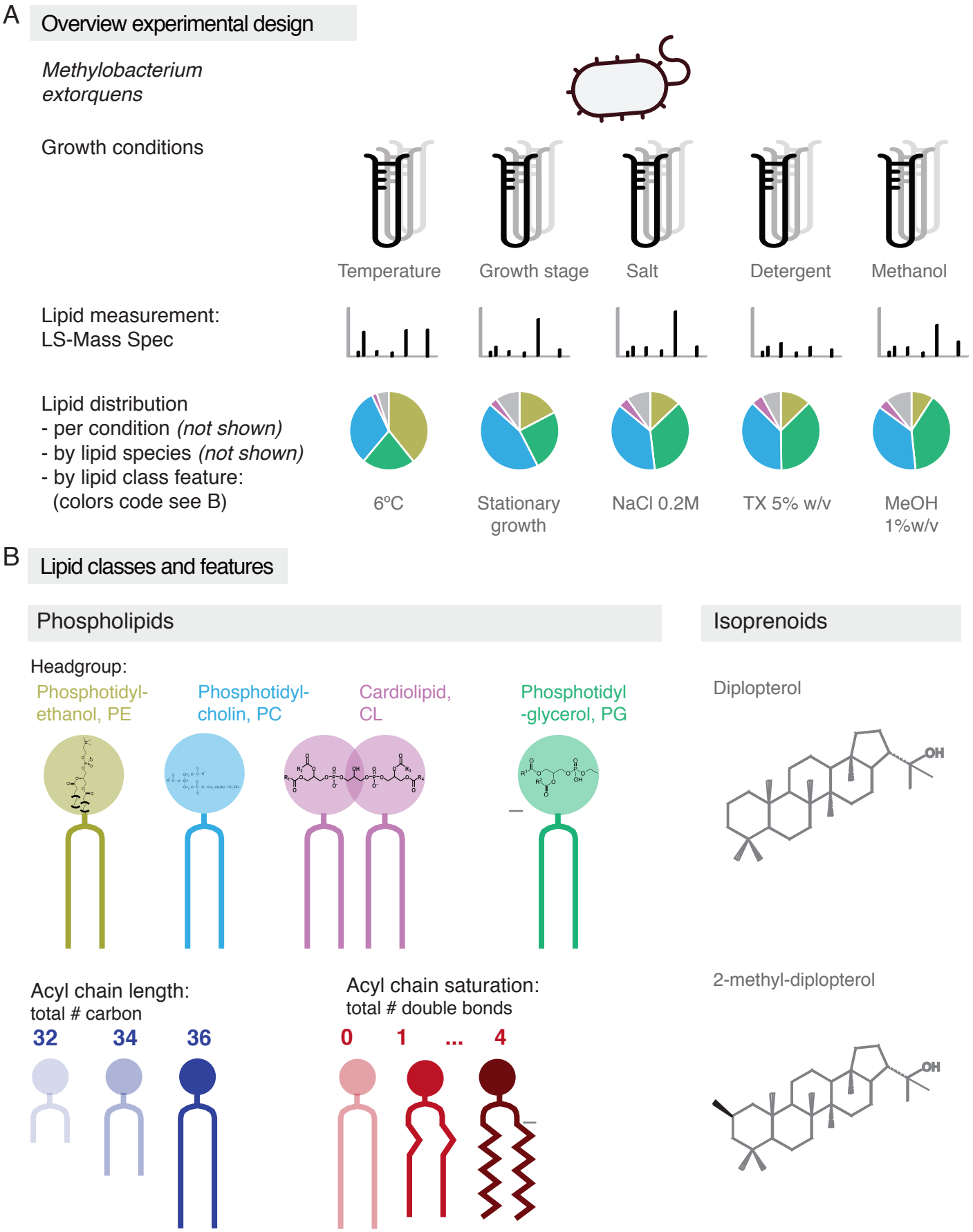

Figure 1. Overview of experimental outline and lipids analysed in this study. (A) Overview of experimental design and exemplary data obtained. **(B)** Schematic of lipid structural features measured in this study: head groups of phosopholipids and isoprenoids, acyl chain length and acyl chain saturation (number of double bonds).

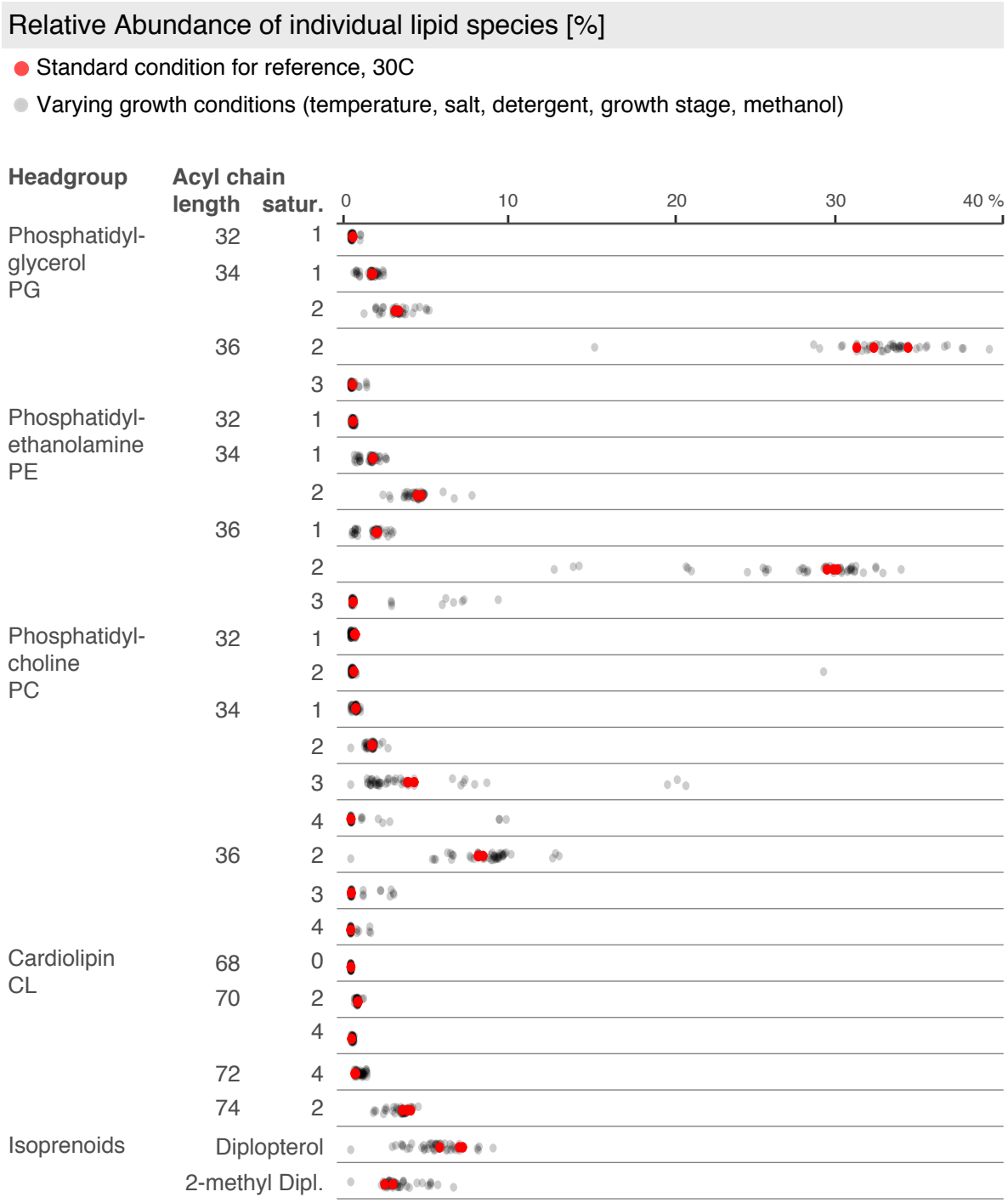

Figure 2. Table of lipid species abundances. Lipid species are annotated by class/head group (PG, PE, PC, CL or diplopterol), total acyl chain length (32 to 74), and total acyl chain saturation (number of double bonds per lipid, 0 to 4). Abundance is shown as percentage of total lipids per experiment. The range in abundance across all experimental conditions is indicated by individual grey dots, the abundances for the standard growth condition (30 ˚C, early exponential stage, 0.15 M sucrose) are shown in red.

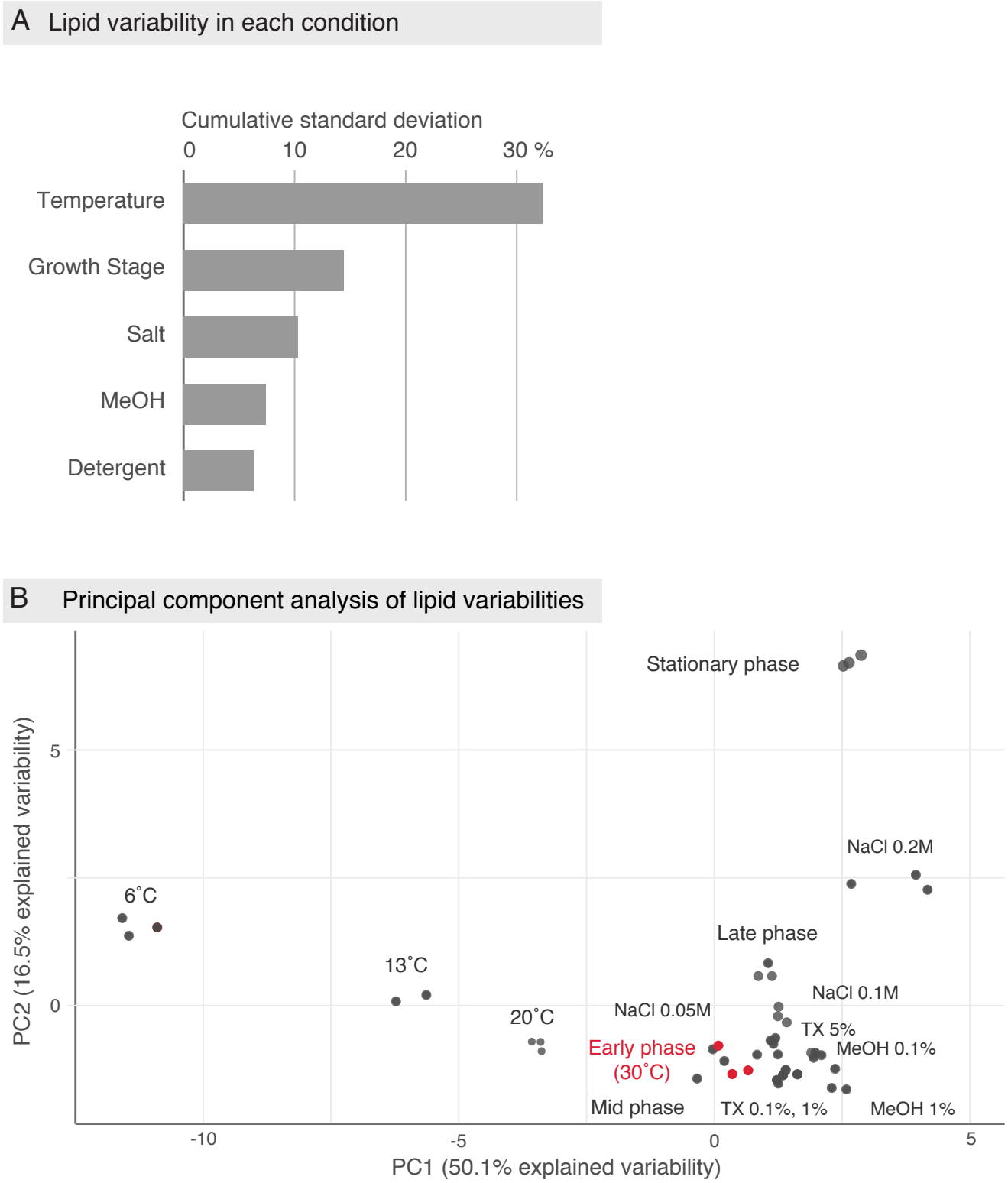

Figure 3. Effect of experimental conditions on lipidomic variability. (A) Total lipidomic variability is given as the cumulative standard deviation of individual lipid species across each set of experimental conditions. Lipid variability is highest when varying temperature, and lowest in increasing percentage of detergent. **(B)** Principle component analysis (PCA) of the lipid species abundances shows the degree of variation between subconditions. The standard growth condition (30 ˚C, early exponential stage, 0.15 M sucrose) is indicated in red, and all other subconditions are grey. Again, lipidomes vary greatly in changing temperatures regimes, and also when bacteria enter stationary phase growth. TX = detergent

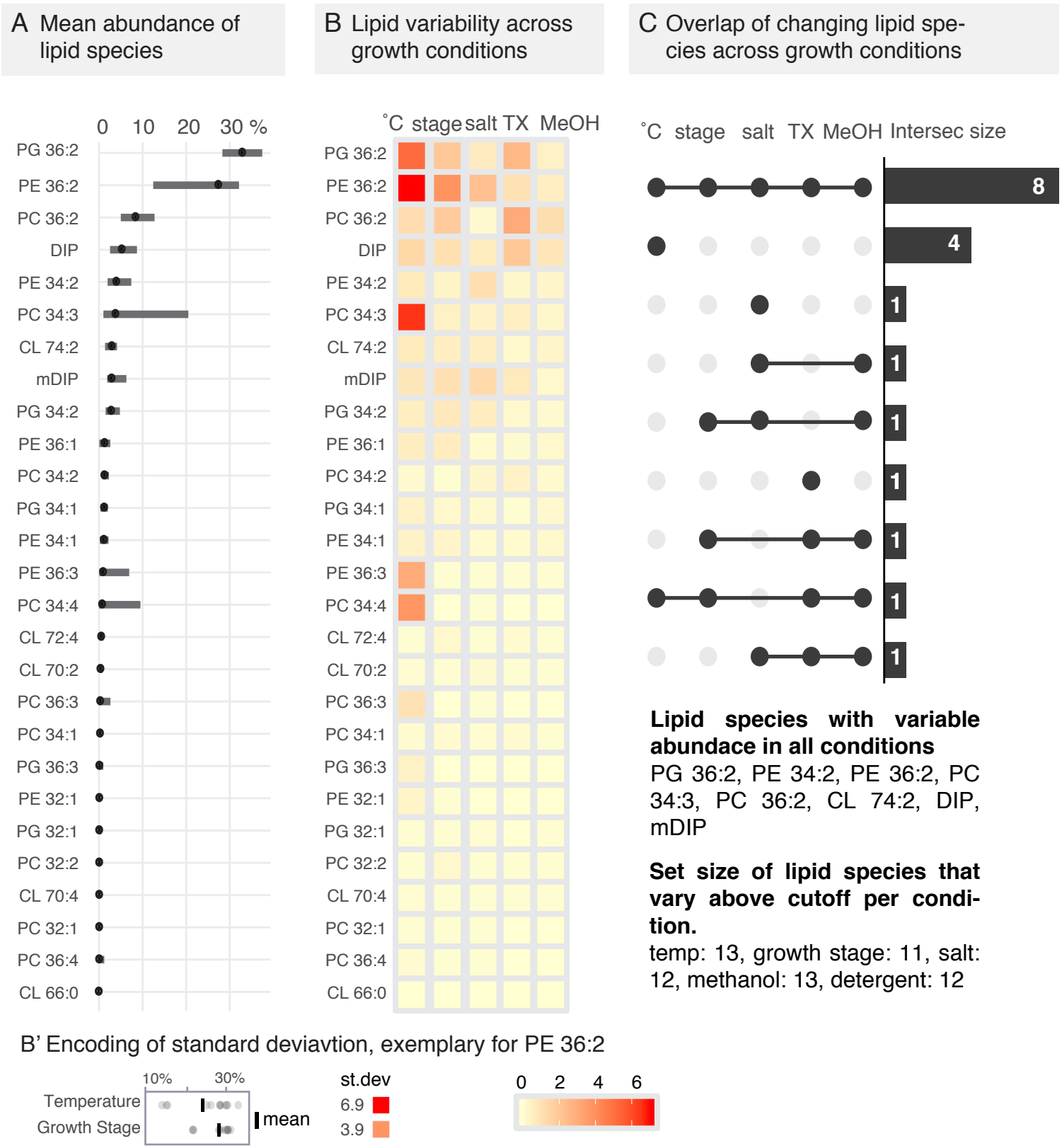

Figure 4. Variability of individual lipid species across experimental conditions. (A) Average abundances of lipid species for all conditions sorted from highest (PG 36:2) to lowest (CL 66:0) lipid species. Mean and range are shown for each lipid. **(B)** Heat map of lipid species variability across experimental conditions, high variability is indicated in red, no variability in light yellow. (B') Exemplary calculation of standard deviation. **(C)** UpSetR plot (Conway, 2017) showing the overlap of lipids adapting their amounts across the experimental conditions. Eight lipids vary their abundance in all experimental conditions, four lipids vary abundance specifically in changing temperatures. stage = growth stage/phase, TX = varying detergent concentrations.

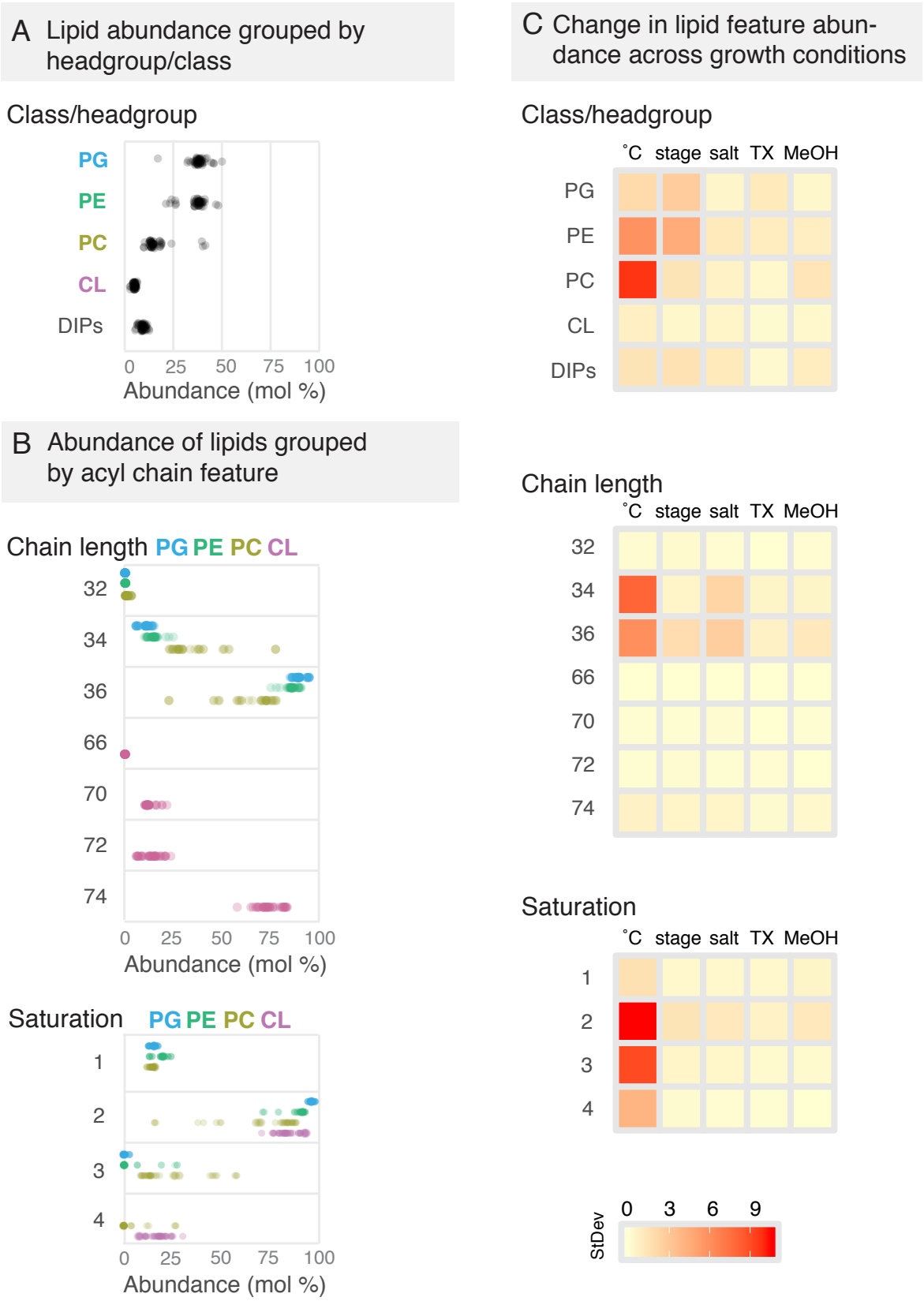

Figure 5. Variability of phospholipid structural features across experimental conditions. **(A)** Abundances of lipids grouped by lipid class shows overall low variability, and lowest variability of CL. **(B)** Abundances of phospholipid headgroup binned by acyl chain length and acyl chain saturation respectively reveals group specific differences in acyl chain remodelling. (headgroups blue = PG, green = PE, olive = PC, magenta = CL). **(A), (B)** each data point shows mean lipid amount from three biological replicates. **(C)** Variability of lipid features plotted for each set of experimental conditions. Stage: bacterial growth stage/phase, TX: varying detergent concentrations.

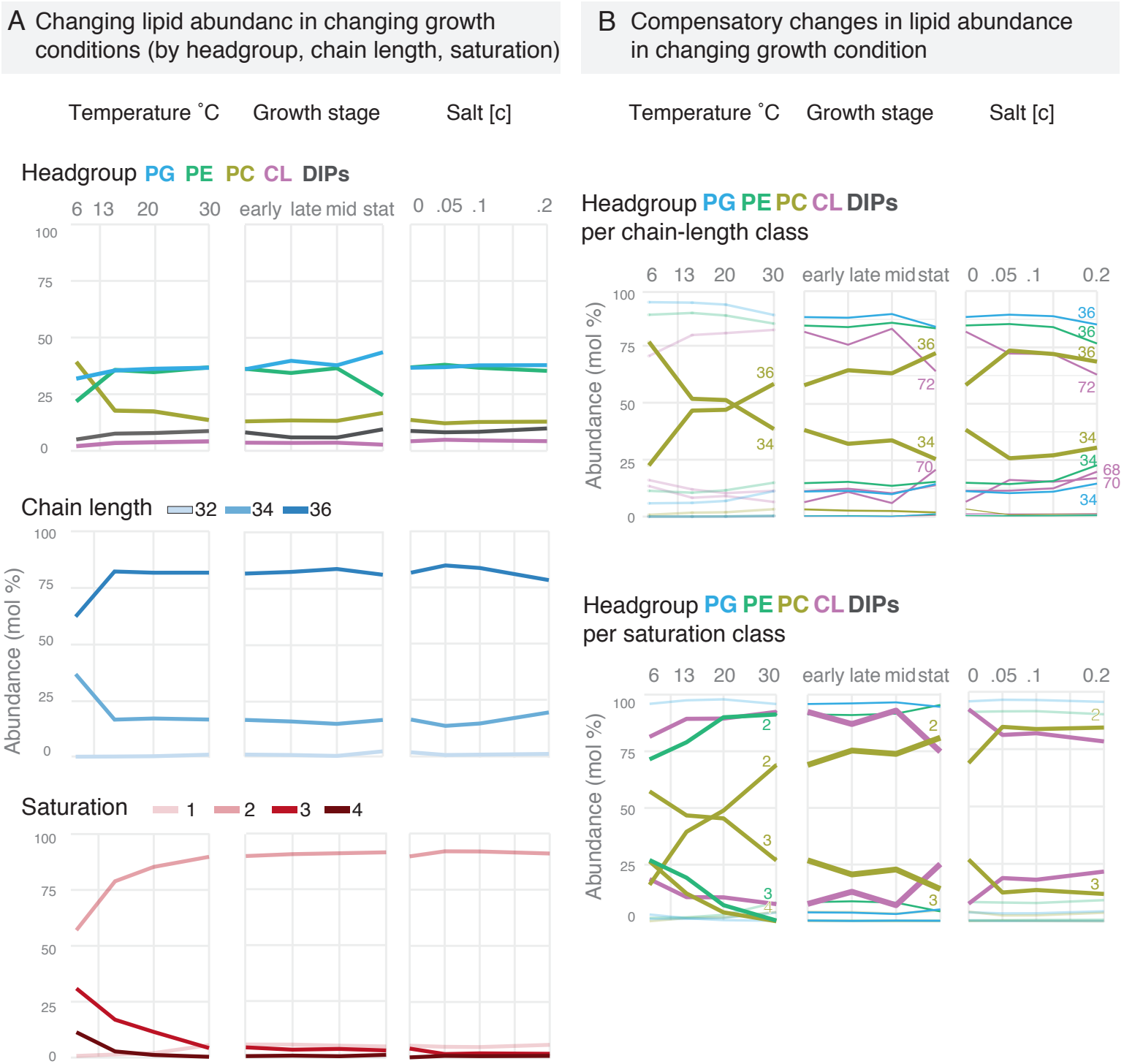

Figure 6. Step-wise adaptation of lipids by feature at changing environmental growth conditions. (A) Abundances of lipids grouped by class, acyl chain length and acyl chain saturation when changing growth temperature, probing at different growth stages, and varying salt (NaCl) concentration of the growth media. **(B)** Abundances of phospholipids grouped by acyl chain features, with headgroups indicated by color (blue: PG, green: PE, olive: PC, magenta: CL). This reveals compensatory effects in lipid adaptability: while abundance of PC with 2 double bonds increases with increasing temperatures, PC with 3 double bonds decreases from 6 to 30 degrees. In each panel, the most variable features are highlighted in bold.

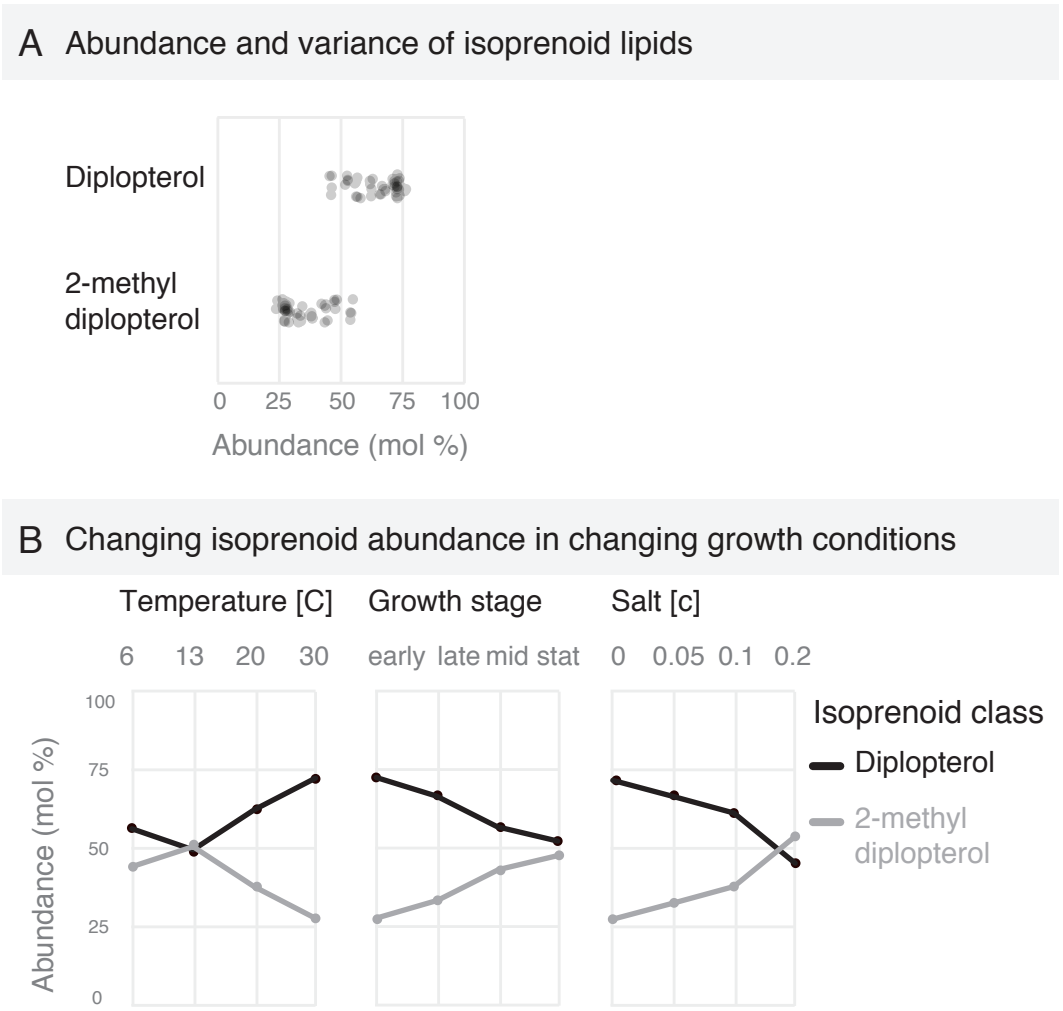

Figure 7. Diplopterol (hopanoid) methylation (A) Abundances of diplopterol species across growth conditions. **(B)** Step-wise adaptation of diplopterols when changing temperature, growth phase, and salt condition.

Methylobacterium extorquens
Gram-negative plant-based model to explore membrane adaptability

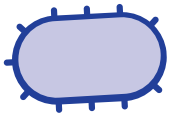

Systematic exploration of diverse enviornmental conditions
The standard growth condition (30°C, early growth phase) was adapted to new regimes.

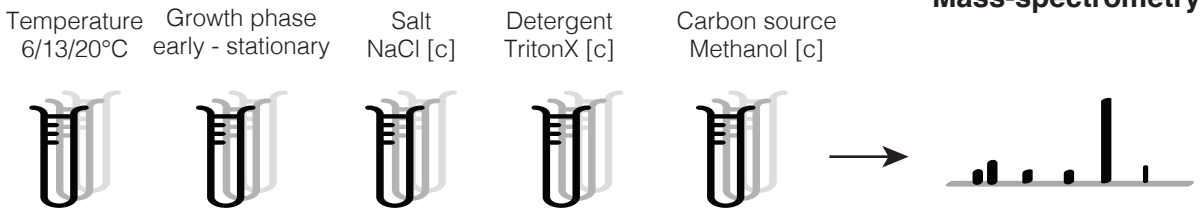

Lipids were identified and meausred by high-resolution **Quantitative Mass-spectrometry**

PCA shows robust lipidome across conditions, remodeling is notable in variable temperature conditions.

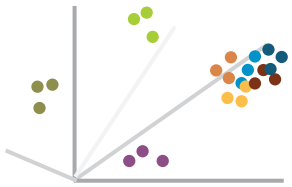

Variability across conditions: 8 lipid species were adapted in all conditions.

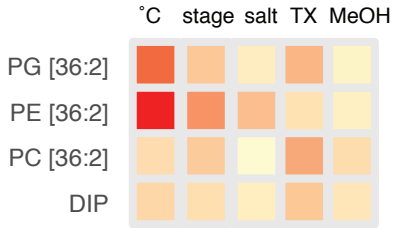

Lipidome composition assessed by lipid feature remodelling (e.g. headgroup, chain length, unsaturation) reveals complex patterns of adaptation in a simple lipidome.

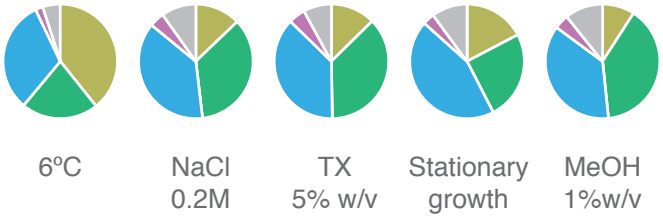

Figure 1 - supplement 1 Graphical abstract

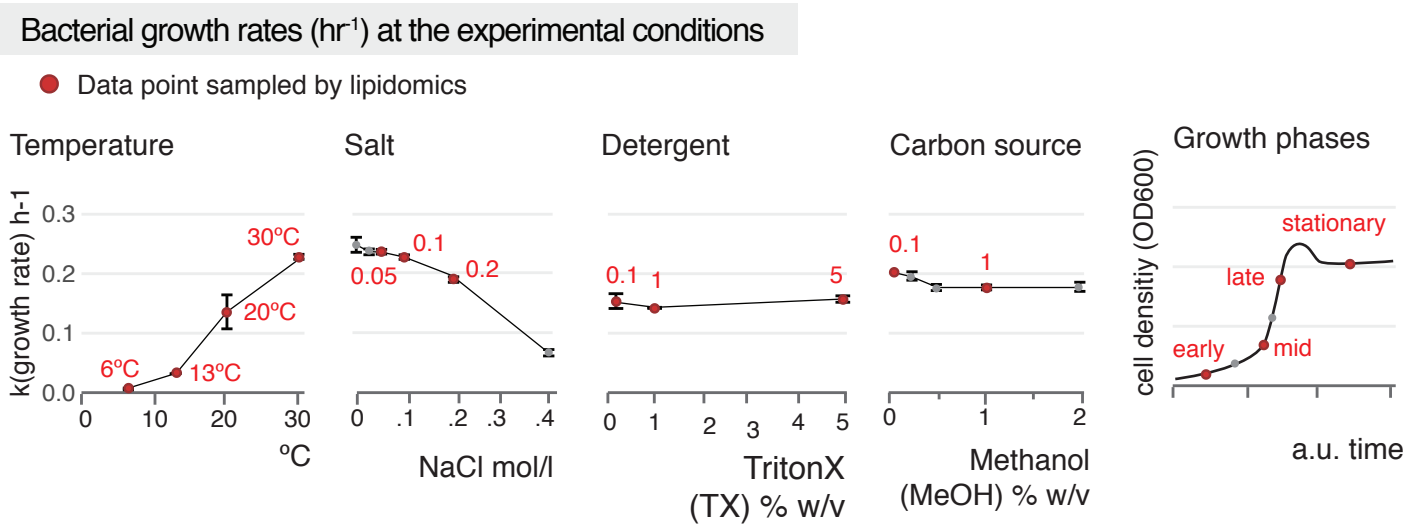

Figure 1 – Supplement 2 Bacterial growth curves and sampling points for lipidomic analysis. Chart for growth phases is a conceptual drawing.

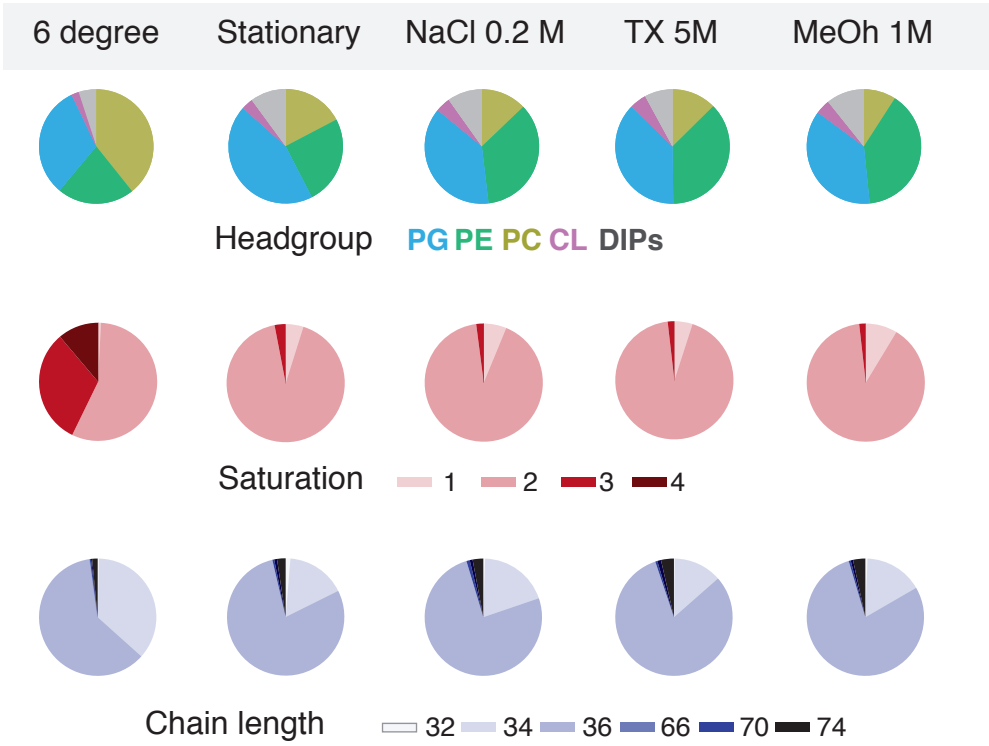

Figure 6 - Supplement 1 Overview of compositional changes across exemplary experimental conditions reveals the lipidome is robust in most growth conditions except in drastic temperature changes when the lipidome is markedly different.

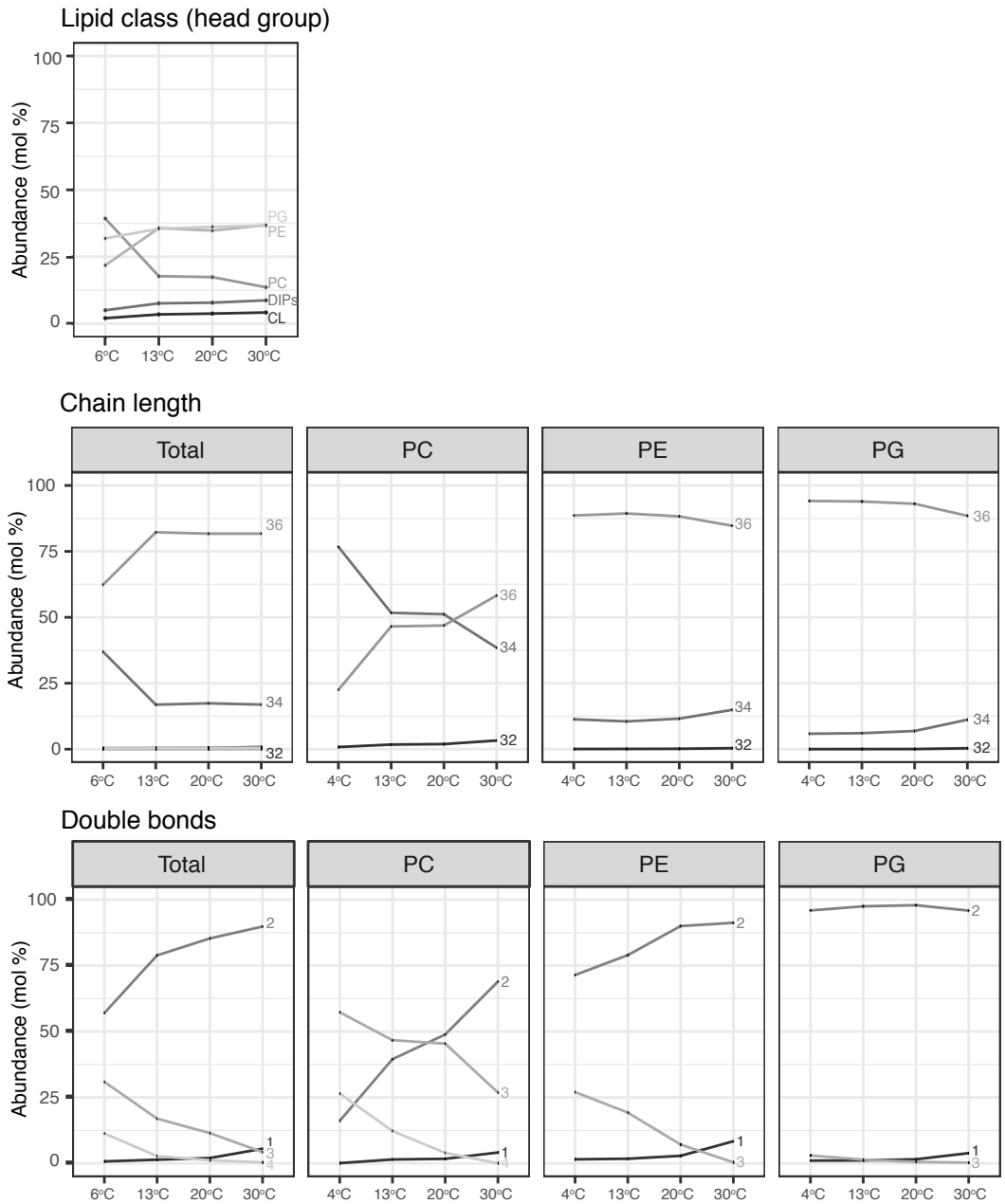

Figure 6 - Supplement 2. Step-wise adaptation of lipids by feature sampled at varying growth temperatures.

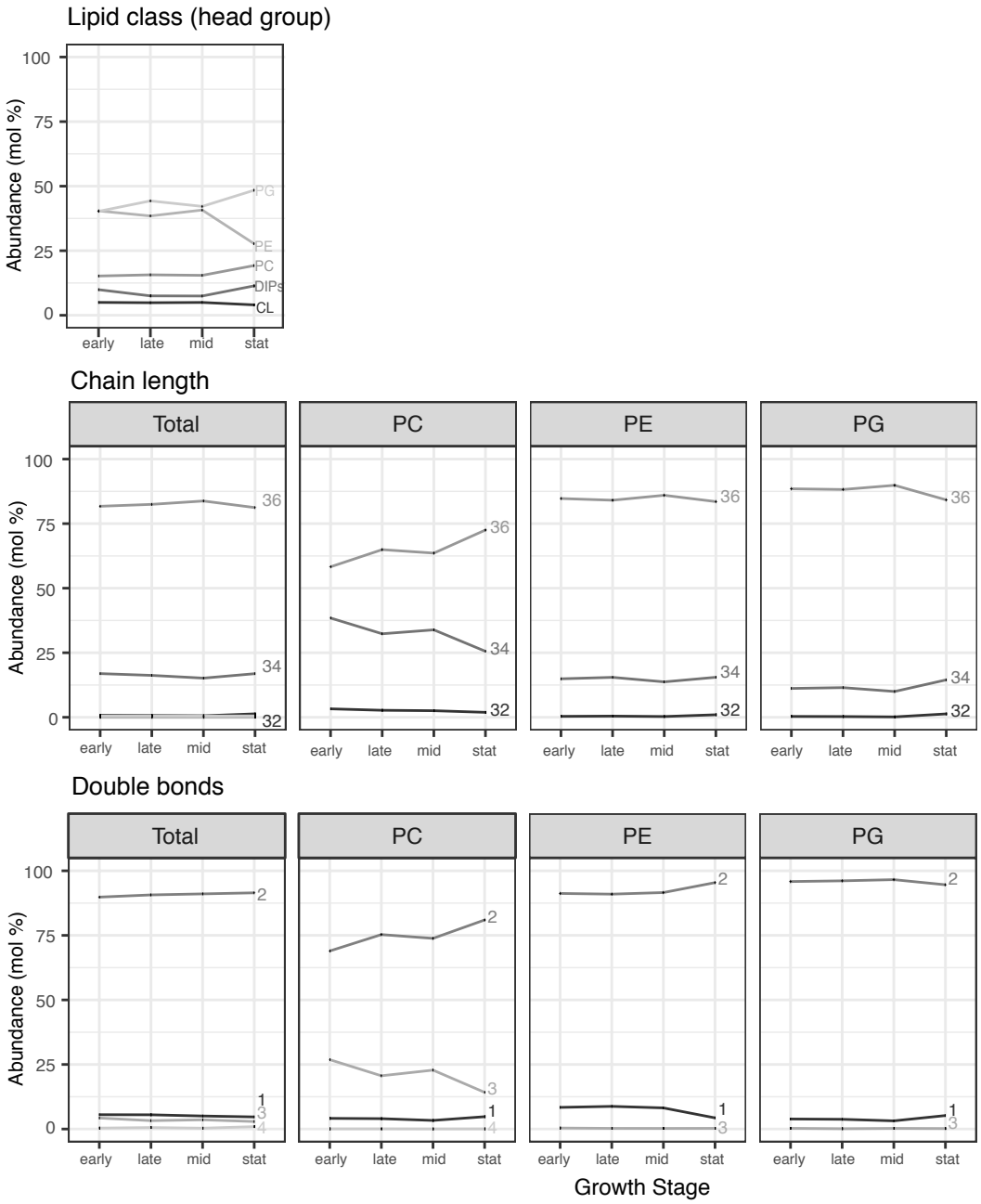

Figure 6 - Supplement 3. Step-wise adaptation of lipids by feature sampled at early, late, mid and stationary growth phase.

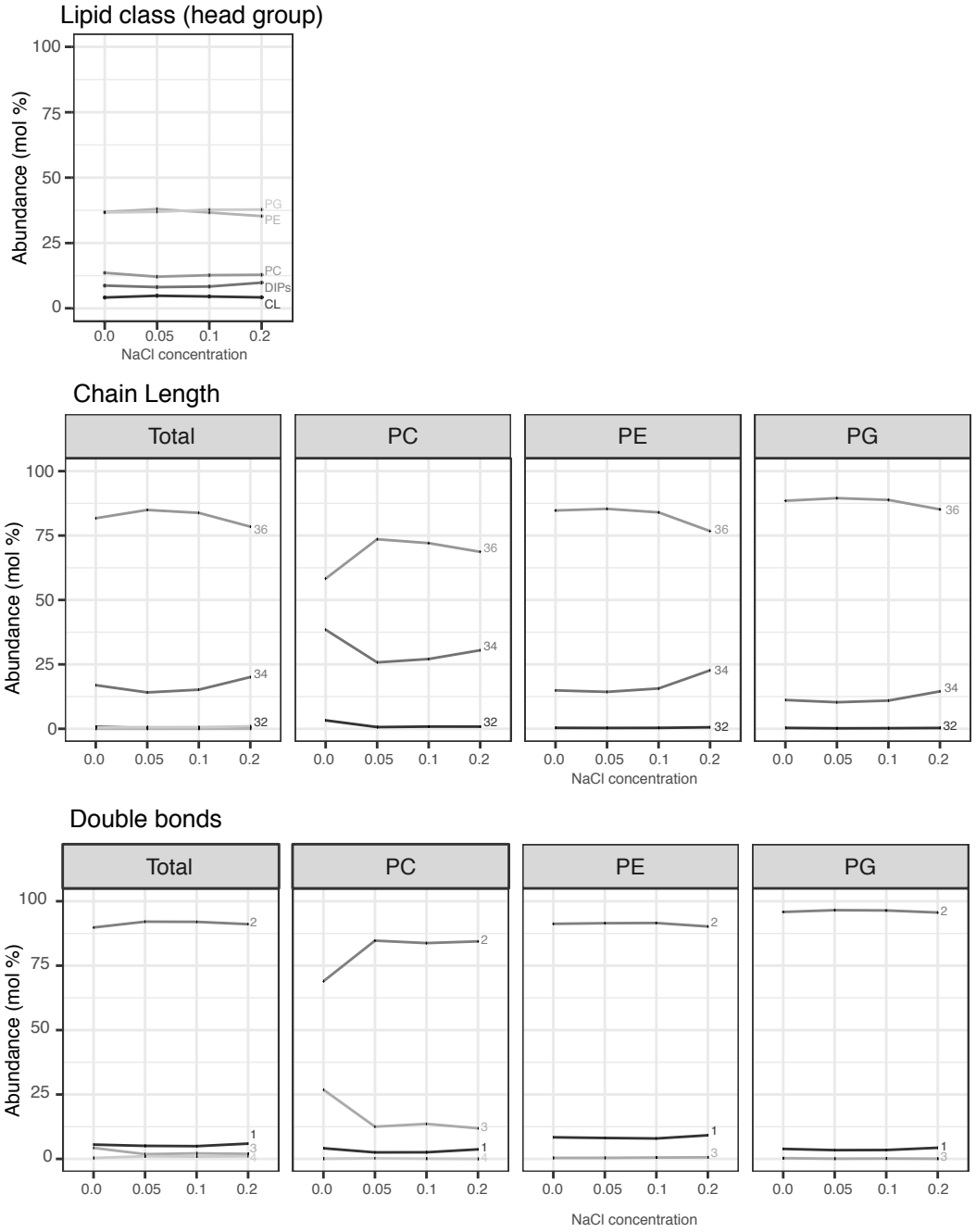

Figure 6 - Supplement 4. Step-wise adaptation of lipids by feature sampled at varying salt concentrations (NaCl).